

SIRT3 regulates mitochondrial fatty-acid oxidation by reversible enzyme deacetylation

Matthew D. Hirschey^{1,2}, Tadahiro Shimazu^{1,2}, Eric Goetzman³, Enxuan Jing⁴, Bjoern Schwer^{1,2,5}, David B. Lombard⁵, Carrie A. Grueter⁶, Charles Harris⁶, Sudha Biddinger⁴, Olga R. Ilkayeva⁷, Robert D. Stevens⁷, Yu Li⁸, Asish K. Saha⁹, Neil B. Ruderman⁹, James R. Bain⁷, Christopher B. Newgard⁷, Robert V. Farese Jr⁶, Frederick W. Alt⁵, C. Ronald Kahn⁴ & Eric Verdin^{1,2}

Sirtuins are NAD⁺-dependent protein deacetylases. They mediate adaptive responses to a variety of stresses, including calorie restriction and metabolic stress. Sirtuin 3 (SIRT3) is localized in the mitochondrial matrix, where it regulates the acetylation levels of metabolic enzymes, including acetyl coenzyme A synthetase 2 (refs 1, 2). Mice lacking both *Sirt3* alleles appear phenotypically normal under basal conditions, but show marked hyperacetylation of several mitochondrial proteins³. Here we report that SIRT3 expression is upregulated during fasting in liver and brown adipose tissues. During fasting, livers from mice lacking SIRT3 had higher levels of fatty-acid oxidation intermediate products and triglycerides, associated with decreased levels of fatty-acid oxidation, compared to livers from wild-type mice. Mass spectrometry of mitochondrial proteins shows that long-chain acyl coenzyme A dehydrogenase (LCAD) is hyperacetylated at lysine 42 in the absence of SIRT3. LCAD is deacetylated in wild-type mice under fasted conditions and by SIRT3 *in vitro* and *in vivo*; and hyperacetylation of LCAD reduces its enzymatic activity. Mice lacking SIRT3 exhibit hallmarks of fatty-acid oxidation disorders during fasting, including reduced ATP levels and intolerance to cold exposure. These findings identify acetylation as a novel regulatory mechanism for mitochondrial fatty-acid oxidation and demonstrate that SIRT3 modulates mitochondrial intermediary metabolism and fatty-acid use during fasting.

Proteomic analysis of mitochondrial proteins revealed the acetylation levels of numerous mitochondrial proteins change during fasting⁴. The dependence of SIRT3 enzymatic activity on NAD⁺ suggests that SIRT3 serves as a metabolic sensor and couples the energy status of the cell with the level of mitochondrial protein acetylation^{5–7}. To explore further a possible role of SIRT3 in regulating metabolism, we monitored the protein expression level of hepatic SIRT3 during fasting in wild-type mice. Although hepatic SIRT3 expression was low under basal conditions, its expression was induced during fasting (Fig. 1a). The increase in SIRT3 protein expression during fasting was concomitant with a relative decrease in the acetylation levels of some mitochondrial proteins (two indicated by arrows in Fig. 1b), suggesting that SIRT3 mediated their deacetylation. In agreement with this model, the same two proteins were hyperacetylated in *Sirt3*^{-/-} mice under basal conditions, and their acetylation levels did not change with fasting when SIRT3 was missing (Fig. 1b). Interestingly, the level of acetylation of other mitochondrial proteins did not change during fasting or in the absence of SIRT3,

demonstrating the selectivity of SIRT3-mediated deacetylation (Fig. 1b). SIRT3 expression was also upregulated in response to fasting in brown adipose tissue but not in the brain, heart or kidney (Supplementary Fig. 2).

Because the liver is an important site of metabolic regulation under fasting conditions, we used a metabolomic approach to screen multiple metabolic pathways. No differences were observed in the levels of 15 amino acids and eight organic acids in livers between fasted

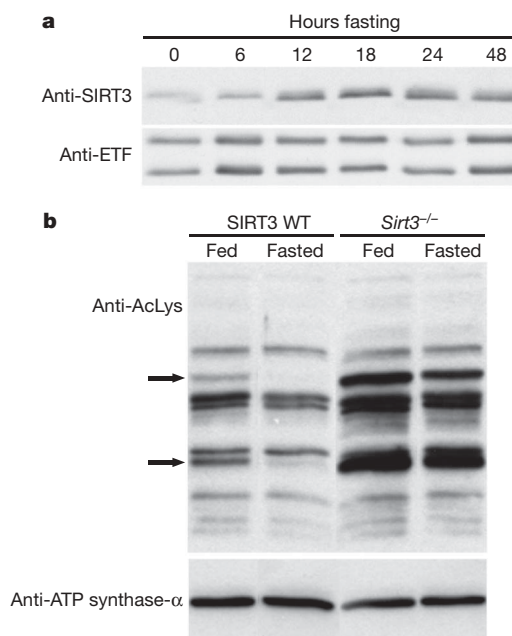


Figure 1 | Fasting induces SIRT3 expression in oxidative tissues.

a, Mitochondria were isolated from livers of fed or fasted (6–48 h) wild-type mice and analysed for SIRT3 expression by western blot analysis; ETF was used as a reference. **b**, Mitochondria isolated from livers of fed or fasted wild-type (WT) and *Sirt3*^{-/-} mice were analysed by western blotting with an antiserum specific for anti-acetyllysine; ATP synthase- α was used as a reference. The arrows identify candidate SIRT3 target proteins that were deacetylated during fasting in wild-type mice, and relatively hyperacetylated and not deacetylated during fasting in *Sirt3*^{-/-} mice.

¹Gladstone Institute of Virology and Immunology, San Francisco, California 94158, USA. ²Department of Medicine, University of California, San Francisco, California 94143, USA. ³Department of Pediatrics, The Children's Hospital of Pittsburgh, University of Pittsburgh School of Medicine, Pittsburgh, Pennsylvania 15201, USA. ⁴Joslin Diabetes Center, Harvard Medical School, Boston, Massachusetts 02215, USA. ⁵Howard Hughes Medical Institute, Program in Cellular and Molecular Medicine, The Children's Hospital, Immune Disease Institute, Department of Genetics, Harvard Medical School, Boston, Massachusetts 02115, USA. ⁶Gladstone Institute of Cardiovascular Disease, University of California San Francisco, California 94158, USA. ⁷Sarah W. Stedman Nutrition and Metabolism Center, Duke University Medical Center, Durham, North Carolina 27704, USA. ⁸Cell Signaling Technology, Danvers, Massachusetts 01923, USA. ⁹Department of Medicine, Physiology, and Biophysics and the Diabetes Unit, Boston University Medical Center, Boston, Massachusetts 02118, USA.

wild-type and *Sirt3*^{-/-} mice (Supplementary Figs 3 and 4, respectively). However, several abnormalities in products of lipid metabolism were found (Fig. 2). Long-chain acylcarnitine species accumulated in the liver (Fig. 2a), but not medium- or short-chain acylcarnitines (data not shown), suggestive of incomplete oxidation of long-chain fatty acids. Analysis of plasma acylcarnitine revealed a striking positive relation between the abundance of acylcarnitines and their chain length: long-chain acylcarnitines (longer than 16 carbon atoms) accumulated in the plasma in *Sirt3*^{-/-} mice and short-chain acylcarnitine species (shorter than 16 carbon atoms) were found in lower amounts compared with wild-type mice

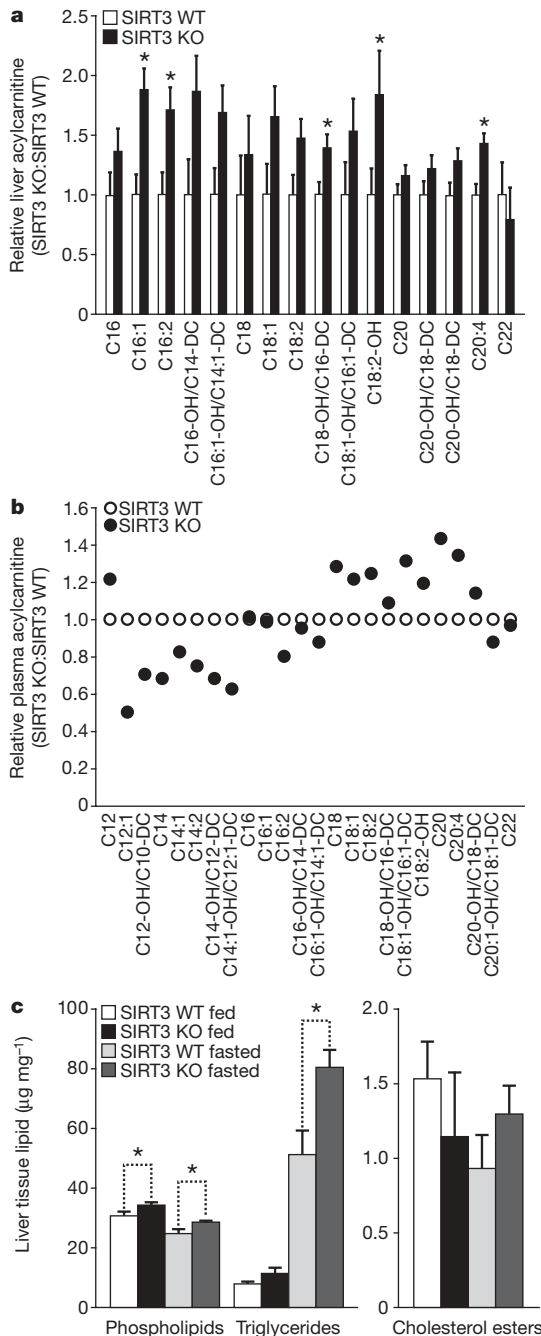


Figure 2 | Abnormal accumulation of acylcarnitines and triglycerides in the livers of mice lacking SIRT3 during fasting. **a**, **b**, Metabolomic analyses were conducted on mouse liver tissue (**a**) and plasma (**b**); data obtained from *Sirt3*^{-/-} mice are shown relative to wild-type mice ($n = 5$ per genotype, fasted 24 h). KO, knockout; **c**, Liver extracts from *Sirt3*^{-/-} and wild-type mice were analysed for total phospholipids, triglycerides and cholesterol esters ($n = 5$ per genotype, fed or fasted 24 h), * $P < 0.05$.

(Fig. 2b and Supplementary Fig. 5). We hypothesized that this trend resulted from the inability of *Sirt3*^{-/-} mice to oxidize long-chain acyl substrates, resulting in their accumulation in plasma. In addition, we predicted reduced oxidation of long-chain acyl substrates in *Sirt3*^{-/-} mice accounts for reduced levels of short-chain acyl substrates. Urinalysis of *Sirt3*^{-/-} mice showed increased urine methylsuccinate, ethylmalonate and isobutyrylglycine, further supporting a defect in fatty-acid oxidation (Supplementary Fig. 6).

In addition, biochemical analysis of tissue revealed increased hepatic triglycerides in *Sirt3*^{-/-} mice (Fig. 2c). Liver triglyceride levels were comparable under fed conditions between wild-type and *Sirt3*^{-/-} mice. Triglyceride levels markedly increased during fasting in wild-type mice, consistent with the mobilization of fatty acids from adipose tissue to the liver. This accumulation was further exacerbated in mice lacking SIRT3 (Fig. 2c), suggesting abnormal fatty-acid metabolism.

Hepatic steatosis is highly correlated with reduced lipid oxidation⁸⁻¹⁰. To assess fatty-acid oxidation directly, *ex vivo* palmitate oxidation was measured in liver homogenates from wild-type and *Sirt3*^{-/-} mice by assessing the rate of conversion of radiolabelled palmitate into either acid-soluble metabolites (Fig. 3a) or CO₂ (Fig. 3b). Under low substrate concentrations, wild-type and *Sirt3*^{-/-} tissue homogenates showed equal abilities to oxidize palmitate (Fig. 3a, b). However, as lipid concentrations increased, we found that liver tissue from fasted *Sirt3*^{-/-} mice had a lower oxidizing capacity than wild-type tissue (Fig. 3a, b). Fatty-acid oxidation was also measured in other oxidizing tissues from fasted mice: significant reductions were observed in cardiac muscle (33% lower in *Sirt3*^{-/-} than wild-type mice), in mixed skeletal muscle (51% lower) and in brown adipose tissue (36% lower) (Fig. 3c). This defect in fatty-acid oxidation appeared to be specific,

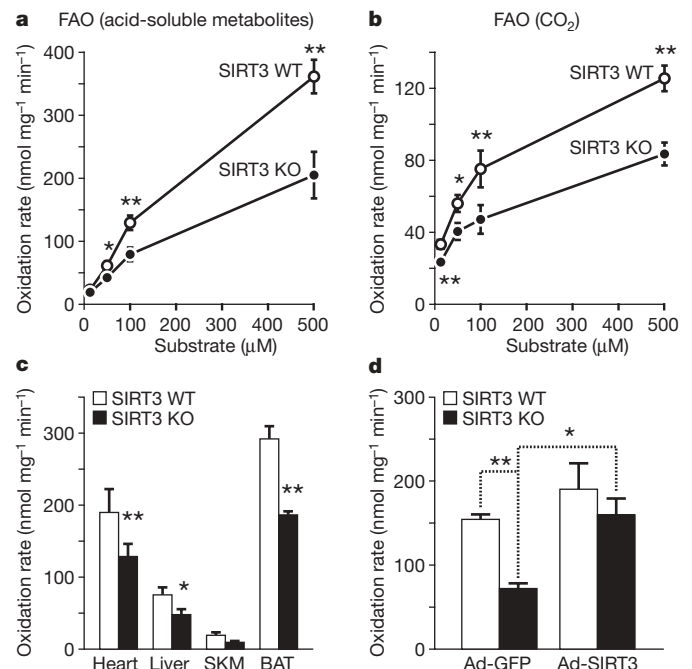


Figure 3 | Defective fatty-acid oxidation in mice lacking *Sirt3*^{-/-}.

a, **b**, Fatty-acid oxidation was measured by incubation of liver extracts from wild-type and *Sirt3*^{-/-} mice with [¹⁴C]palmitate, acid-soluble metabolites (**a**) and captured CO₂ (**b**) ($n = 10$ per genotype). **c**, Mitochondrial fatty-acid oxidation was measured in other oxidizing tissues, including heart, liver, mixed gastrocnemius and soleus skeletal muscle (SKM), and brown adipose tissue (BAT) (CO₂, $n = 7$ per genotype, 100 μM substrate). **d**, Fatty-acid oxidation was measured by incubation of [¹⁴C]palmitate (100 μM) in liver extract from wild-type and *Sirt3*^{-/-} mice one week after injection with recombinant adenovirus expressing GFP or SIRT3 (acid-soluble metabolites, $n = 3-4$ per category). * $P < 0.05$, ** $P < 0.01$.

because citrate synthase activity, a key enzyme of the Krebs cycle and indicator of mitochondrial function, was comparable in wild-type and *Sirt3*^{-/-} mice (Supplementary Fig. 7a). Additionally, mitochondria from *Sirt3*^{-/-} mice were morphologically similar to wild-type mitochondria, as observed by electron microscopy (Supplementary Fig. 7b, c). Because other abnormalities in lipid metabolism could contribute to hepatic steatosis, we directly measured lipogenesis and fatty-acid uptake in primary hepatocytes from wild-type and *Sirt3*^{-/-} mice; however, we observed no differences (Supplementary Fig. 8a, b, respectively). Additionally, no differences were measured in hepatic very-low-density lipoprotein export between wild-type and *Sirt3*^{-/-} mice (Supplementary Fig. 8c). These data support the model that mice lacking SIRT3 develop hepatic steatosis as a result of a unique defect in fatty-acid oxidation. To determine whether reduced fatty-acid oxidation in *Sirt3*^{-/-} mice was cell autonomous, recombinant adenovirus overexpressing SIRT3, or green fluorescent protein (GFP) as a control, were injected into the tail veins of wild-type and *Sirt3*^{-/-} mice. Homogenates of hepatic tissue were collected and assessed for palmitate oxidation. We found an approximate 50% reduction in fatty-acid oxidation between wild-type and *Sirt3*^{-/-} mice after injection of GFP-expressing adenovirus (Fig. 3d), consistent with our previous findings (Fig. 3a). In contrast, we found no difference in palmitate oxidation between wild-type and *Sirt3*^{-/-} mice after injection of SIRT3-expressing adenovirus (Fig. 3d). Furthermore, we found only a modest increase in palmitate oxidation in wild-type mice after SIRT3-overexpression (Fig. 3d). These data demonstrate that the reduction in fatty-acid oxidation observed in mice lacking SIRT3 is a direct result of the absence of SIRT3 in liver, and can be mitigated by exogenous SIRT3 overexpression.

Based on reduced palmitate oxidation and because long-chain acylcarnitines accumulated in the liver and plasma of *Sirt3*^{-/-} mice, we hypothesized that acetylation regulates the activity of key enzymes involved in long-chain fatty-acid degradation. To identify possible SIRT3 targets and to define further the mechanism by which hyperacetylation of mitochondrial proteins results in reduced fatty-acid oxidation, purified hepatic mitochondria were isolated from *Sirt3*^{-/-} mice. They were then subjected to proteolytic digestion (trypsin), immunoprecipitated by anti-acetyllysine antiserum, and analysed by nanoflow liquid chromatography tandem mass spectrometry and ion-trap mass spectrometry. One key enzyme involved in the oxidation of long-chain substrates was identified, LCAD, which contained eight acetylation sites (Supplementary Fig. 9).

Next, we assessed the acetylation level of hepatic LCAD. Endogenous mitochondrial proteins were immunoprecipitated with anti-acetyllysine antiserum and analysed by western blotting using antisera specific for LCAD. This experiment demonstrated LCAD was acetylated and became deacetylated during fasting in wild-type mice (Fig. 4a). When the same experiment was conducted using mitochondria from *Sirt3*^{-/-} mice, LCAD was relatively hyperacetylated in the fed state and not deacetylated during fasting, demonstrating that SIRT3 is necessary for LCAD deacetylation during fasting (Fig. 4a).

To test the ability of SIRT3 to deacetylate LCAD directly, expression vectors encoding Flag-tagged murine LCAD were cotransfected with an expression vector for either SIRT3, SIRT3-H248Y (a catalytically inactive SIRT3 mutant), SIRT4 or SIRT5 into HEK-293 cells. Acetylation levels for murine LCAD were measured after immunoprecipitation (anti-Flag) by western blotting with anti-acetyllysine antiserum. SIRT3, but not SIRT3-H248Y, SIRT4 or SIRT5, deacetylated LCAD (Fig. 4b). Additionally, to measure the ability of SIRT3 to deacetylate LCAD *in vitro* directly, recombinant LCAD purified after overexpression in *Escherichia coli* was incubated with recombinant SIRT3 wild-type or SIRT3-H248Y. Recombinant LCAD was probed for changes in acetylation by western blotting with anti-acetyllysine antiserum. SIRT3, but not SIRT3-H248Y, deacetylated LCAD *in vitro* (Fig. 4c). We also tested whether SIRT3 could directly interact with LCAD by co-immunoprecipitation. We found both SIRT3 and SIRT3-H248Y, but not SIRT4 and SIRT5, interacted with LCAD

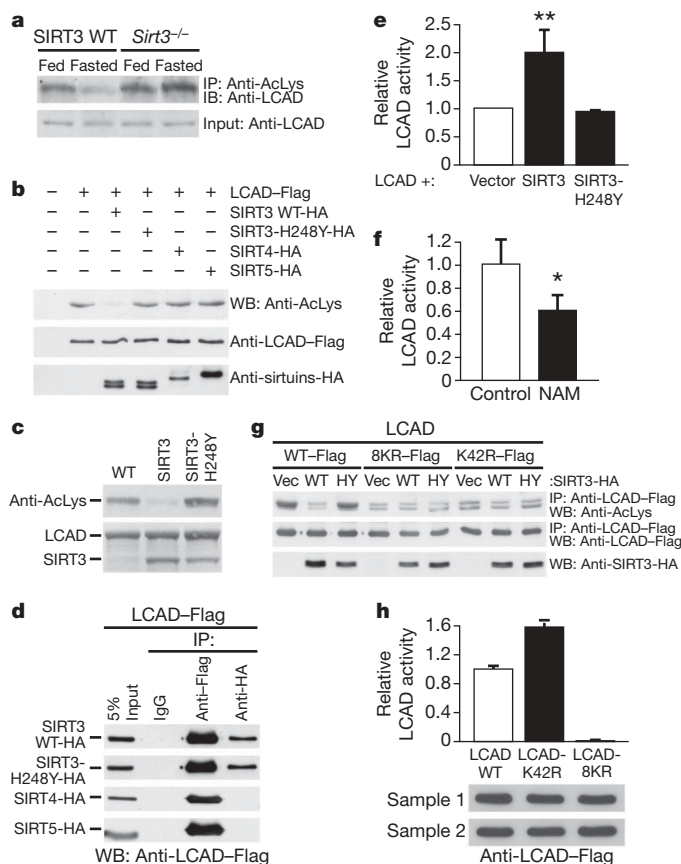


Figure 4 | LCAD is hyperacetylated in *Sirt3*^{-/-} mice, deacetylated by SIRT3 *in vivo* and *in vitro*, and displays increased enzymatic activity when deacetylated. **a**, Liver extracts from wild-type and *Sirt3*^{-/-} mice (fed or fasted) were immunoprecipitated with an anti-acetyllysine antiserum and analysed with anti-LCAD antiserum. IB, immunoblot. **b**, Expression vectors for wild-type SIRT3, SIRT3-H248Y (catalytically inactive SIRT3 mutant), SIRT4 or SIRT5 were co-transfected with expression vectors for Flag-tagged LCAD, and the level of LCAD acetylation assessed. HA, haemagglutinin tagged. **c**, Recombinant LCAD expressed in *E. coli* was incubated *in vitro* with recombinant SIRT3 or SIRT3-H248Y, and the status of LCAD acetylation assessed. **d**, Expression vectors for wild-type SIRT3, SIRT3-H248Y, SIRT4 and SIRT5 (HA-tagged) were co-transfected with expression vectors for Flag-tagged LCAD and assessed for interaction by co-immunoprecipitation. **e**, LCAD was expressed, purified, and incubated with SIRT3 or SIRT3-H248Y and its enzymatic activity measured *in vitro* using 2,6-dimethylheptanoyl-CoA as a substrate ($n = 4$ independent assays). **f**, Recombinant LCAD was expressed in *E. coli* in the absence (control) or presence of nicotinamide (NAM, 50 mM), purified and its enzymatic activity measured *in vitro* using 2,6-dimethylheptanoyl-CoA as a substrate ($n = 4$ independent assays). **g**, Expression vectors for wild-type LCAD, LCAD single acetylation-point mutant (LCAD-K42R) or LCAD eight acetylation-point mutant (LCAD-8KR) were co-transfected with expression vectors for wild-type SIRT3 or SIRT3-H248Y, and the level of acetylation assessed. **h**, Wild-type LCAD, LCAD-K42R or LCAD-8KR were expressed in HEK-293 cells and measured for enzymatic activity *in vitro* using 2,6-dimethylheptanoyl-CoA as a substrate ($n = 5$ measurements per sample; error bars represent data from two independent protein purifications). * $P < 0.05$, ** $P < 0.01$.

(Fig. 4d). To determine whether SIRT3 could deacetylate human LCAD with a similar ability as murine LCAD, we measured deacetylation *in vitro* and *in vivo* and found it effectively did so (Supplementary Fig. 10). Although the role of human LCAD in fatty-acid oxidation is incompletely understood, the high sequence homology between mouse and human LCAD (Supplementary Fig. 10), the robust expression level of LCAD in human liver¹¹, and similar tissue expression patterns between LCAD and other fatty-acid oxidation enzymes¹¹ suggest an important role for LCAD in fatty-acid oxidation in humans, as in mice.

To determine whether the acetylation state of LCAD modified its enzymatic activity, LCAD was overexpressed in HEK-293 with SIRT3 or with SIRT3-H248Y, purified by immunoprecipitation and assayed for LCAD enzymatic activity using 2,6-dimethylheptanoyl-CoA, a highly specific substrate for LCAD. Co-expression of LCAD with SIRT3 induced LCAD deacetylation (Fig. 4b), and a twofold increase in enzymatic activity was observed (Fig. 4e). However, when LCAD was overexpressed in the presence of SIRT3-H248Y, enzymatic activity was similar to basal levels observed with LCAD only (Fig. 4e). We also overexpressed recombinant LCAD in *E. coli* with or without nicotinamide (50 mM), which induced its hyperacetylation, as reported for acetyl-CoA synthetase 2 (ref. 1), and observed that hyperacetylated LCAD showed an approximate 40% reduction in enzymatic activity (Fig. 4f).

To determine which of the eight identified acetylated lysine residues on LCAD were targets of SIRT3, we analysed semiquantitative mass spectrometry data. We found that LCAD lysine 42 was significantly hyperacetylated in *Sirt3*^{-/-} compared with wild-type mice (a greater than 20-fold increase) (Supplementary Fig. 10). Expression vectors for a single-site mutant LCAD (LCAD-K42R) and for an eight-site mutant LCAD (mutating lysine residues 42, 156, 189, 240, 254, 318, 322 and 358, LCAD-8KR) were generated, transfected in HEK-293 cells and assayed for acetylation and enzymatic activity. Both mutants, LCAD-8KR and LCAD-K42R, were notably less acetylated than wild-type LCAD under basal conditions and were not (LCAD-8KR) or minimally (LCAD-K42R) further deacetylated by SIRT3 (Fig. 4g). Interestingly, the LCAD-8KR mutant showed only a small reduction in acetylation compared with LCAD-K42R (Fig. 4g), supporting the model that lysine 42 is the major site of acetylation in LCAD.

Finally, to measure the effect of constitutive deacetylation in the single-site (LCAD-K42R) and eight-site (LCAD-8KR) LCAD mutants on their enzymatic activity, we purified both proteins by immunoprecipitation (anti-Flag) after overexpression in HEK-293 cells. We found a significant increase in enzymatic activity of the LCAD-K42R protein compared with wild-type LCAD (Fig. 4h). However, no residual enzymatic activity was measured in the mutant LCAD-8KR (Fig. 4h). These data identify LCAD lysine 42 as a critical lysine residue for the regulation of LCAD enzymatic activity. Because lysine 42 is also the primary site of LCAD acetylation and is regulated by SIRT3, these observations are consistent with the model that SIRT3 regulates LCAD enzymatic activity by the deacetylation of lysine 42.

Finally, we further explored the consequence of decreased fatty-acid oxidation in *Sirt3*^{-/-} mice on hepatic ATP levels during fasting. In agreement with the defect in fatty-acid oxidation described earlier in *Sirt3*^{-/-} mice, we found hepatic ATP levels to be significantly lower in fasted *Sirt3*^{-/-} mice (43% reduction) than wild-type mice (Fig. 5a). These data further support a recent observation describing reduced ATP levels in multiple highly oxidizing tissues in *Sirt3*^{-/-} mice¹². We measured additional metabolic parameters in *Sirt3*^{-/-} mice under fed and fasted conditions, including glucose and free fatty acids, and found no differences compared with wild-type mice (Supplementary Table 1). However, measurements of ketone bodies under fasting conditions revealed reduced β -hydroxybutyrate (15% reduction) in *Sirt3*^{-/-} mice, consistent with reduced fatty-acid oxidation (Supplementary Table 1).

Cold exposure is another metabolic stress associated with enhanced fatty-acid oxidation, and reduced cold tolerance is a common feature of fatty-acid oxidation deficiency in mice^{13,14}. Accordingly, *Sirt3*^{-/-} mice exhibited a striking cold intolerance during fasting (Fig. 5b). In contrast, fed *Sirt3*^{-/-} mice showed cold tolerance comparable to wild-type mice (Fig. 5b). Previous studies have established a link between reduced fatty-acid oxidation and glucose metabolism^{15,16}. We therefore assessed glucose levels during cold exposure. Plasma glucose levels increased similarly in fed *Sirt3*^{-/-} and wild-type mice during cold exposure (Fig. 5c). However, when fasted, *Sirt3*^{-/-} mice

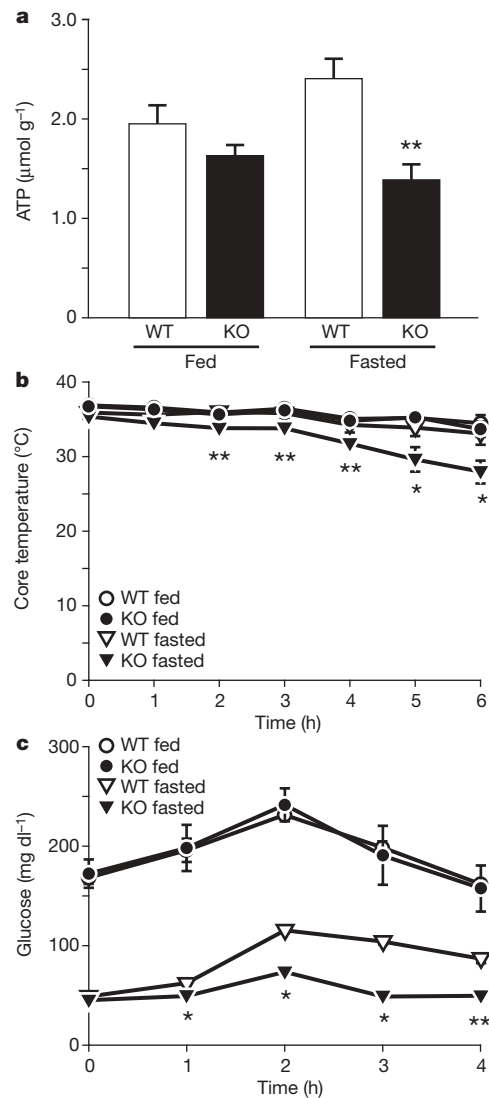


Figure 5 | Mice lacking SIRT3 show reduced ATP production, cold intolerance and hypoglycaemia. **a**, Hepatic ATP levels were measured in fed and fasted wild-type and *Sirt3*^{-/-} mice ($n = 5$ per genotype per condition). **b**, **c**, Core temperature (**b**) and blood glucose (**c**) were measured in fed and fasted wild-type and *Sirt3*^{-/-} mice exposed to cold (4 °C) for 6 h ($n = 5$ per genotype per condition). * $P < 0.05$, ** $P < 0.01$.

showed almost no increase in plasma glucose in response to cold (9% increase) compared with wild-type mice (119% increase) (Fig. 5c). We postulate that reduced glucose in cold-challenged *Sirt3*^{-/-} mice is caused by decreased fatty-acid oxidation, and reduced ATP available for gluconeogenesis^{15,16}. Together, these observations identify a novel metabolic regulatory mechanism for fatty-acid oxidation based on the reversible deacetylation of a key fatty-acid oxidation enzyme by the sirtuin SIRT3.

Previously, SIRT3 was proposed to have a role in metabolic regulation based on two prominent findings. First, reduced SIRT3 protein expression has been observed in metabolic disorders, such as leptin insufficiency¹⁷ and type II diabetes¹⁸. Second, SIRT3 requires NAD⁺ as a cofactor¹⁹, which couples its enzymatic activity with the metabolic state of the cell. Thus SIRT3 would be enzymatically more active when the NAD⁺/NADH ratio is high, which has been previously reported to occur in response to metabolic stress²⁰. Conversely, when the NAD⁺/NADH ratio is low, SIRT3 enzymatic activity is expected to be low. The direct requirement for NAD⁺ by SIRT3 could therefore serve as a sensitive, fast-acting sensor of the metabolic state, and positions SIRT3 to respond to cellular energy fluctuations by changes in its enzymatic activity.

Because the fatty-acid oxidation pathway is a major contributor to the regulation of cellular energy balance, especially during fasting^{21,22}, the upregulation of SIRT3 expression and the increase in cellular NAD⁺ that both occur during the transition to fasting²⁰ could work in synergy to maximally induce SIRT3 deacetylation of LCAD-K42, and subsequent increases in LCAD activity and fatty-acid oxidation output.

We demonstrate that increased SIRT3 expression and activity deacetylates and enzymatically activates the fatty-acid oxidation enzyme LCAD. The abundance of acetylated mitochondrial proteins⁴ suggests that other mitochondrial proteins in the fatty-acid oxidation pathway could be regulated by reversible acetylation and might be targets of SIRT3 or other mitochondrial sirtuins. Whether *Sirt3*^{-/-} mice are sensitive to other conditions where energy demand is high, or have metabolic defects in additional oxidative tissues, remains unknown. Because inhibitors or genetic lesions in the fatty-acid oxidation pathway are associated with several metabolic disorders, including diabetes²³, cardiovascular disease²⁴ and steatosis/steatohepatitis²⁵, future experiments will examine the possible pathogenic role of SIRT3 in these conditions and address the potential therapeutic value of enhancing SIRT3 activity in these disorders.

METHODS SUMMARY

Antibodies used were specific for ATP synthase subunits α and β (Invitrogen Molecular Probes), monoclonal and polyclonal acetyllysine (Cell Signaling Technology), SIRT3 (as described³), electron transfer flavoprotein (ETF) and LCAD (provided by J. Vockley). Oxidation of [1-¹⁴C]palmitic acid by tissue homogenate was adapted from a previously established method²⁶. Briefly, tissue was homogenized in sucrose/Tris/EDTA buffer, incubated for 30–60 min in the reaction mixture (pH 8.0) containing [1-¹⁴C]palmitic acid, and measured for acid-soluble metabolites and trapped CO₂. Enzymatic activity for LCAD was measured by the anaerobic ETF fluorescence reduction assay²⁷, using 2,6-dimethylheptanoyl-CoA as a substrate in recombinant LCAD expressed and purified from HEK-293T cells with wild-type or catalytically inactive SIRT3, or in *E. coli* in the absence (control) or presence of nicotinamide (50 mM)²⁸.

Full Methods and any associated references are available in the online version of the paper at www.nature.com/nature.

Received 17 December 2008; accepted 21 December 2009.

- Schwer, B., Bunkenborg, J., Verdin, R. O., Andersen, J. S. & Verdin, E. Reversible lysine acetylation controls the activity of the mitochondrial enzyme acetyl-CoA synthetase 2. *Proc. Natl Acad. Sci. USA* **103**, 10224–10229 (2006).
- Hallows, W. C., Lee, S. & Denu, J. M. Sirtuins deacetylate and activate mammalian acetyl-CoA synthetases. *Proc. Natl Acad. Sci. USA* **103**, 10230–10235 (2006).
- Lombard, D. B. et al. Mammalian Sir2 homolog SIRT3 regulates global mitochondrial lysine acetylation. *Mol. Cell Biol.* **27**, 8807–8814 (2007).
- Kim, S. C. et al. Substrate and functional diversity of lysine acetylation revealed by a proteomics survey. *Mol. Cell* **23**, 607–618 (2006).
- Guarente, L. Sirtuins as potential targets for metabolic syndrome. *Nature* **444**, 868–874 (2006).
- Schwer, B. & Verdin, E. Conserved metabolic regulatory functions of sirtuins. *Cell Metab.* **7**, 104–112 (2008).
- Schwer, B. et al. Calorie restriction alters mitochondrial protein acetylation. *Aging Cell* **8**, 604–606 (2009).
- Cox, K. B. et al. Gestational, pathologic and biochemical differences between very long-chain acyl-CoA dehydrogenase deficiency and long-chain acyl-CoA dehydrogenase deficiency in the mouse. *Hum. Mol. Genet.* **10**, 2069–2077 (2001).
- Kurtz, D. M. et al. Targeted disruption of mouse long-chain acyl-CoA dehydrogenase gene reveals crucial roles for fatty acid oxidation. *Proc. Natl Acad. Sci. USA* **95**, 15592–15597 (1998).
- Zhang, D. et al. Mitochondrial dysfunction due to long-chain Acyl-CoA dehydrogenase deficiency causes hepatic steatosis and hepatic insulin resistance. *Proc. Natl Acad. Sci. USA* **104**, 17075–17080 (2007).

- Son, C. G. et al. Database of mRNA gene expression profiles of multiple human organs. *Genome Res.* **15**, 443–450 (2005).
- Ahn, B. H. et al. A role for the mitochondrial deacetylase Sirt3 in regulating energy homeostasis. *Proc. Natl Acad. Sci. USA* **105**, 14447–14452 (2008).
- Schuler, A. M. & Wood, P. A. Mouse models for disorders of mitochondrial fatty acid beta-oxidation. *ILAR J* **43**, 57–65 (2002).
- Tolwani, R. J. et al. Medium-chain acyl-CoA dehydrogenase deficiency in gene-targeted mice. *PLoS Genet.* **1**, e23 (2005).
- Herrema, H. et al. Disturbed hepatic carbohydrate management during high metabolic demand in medium-chain acyl-CoA dehydrogenase (MCAD)-deficient mice. *Hepatology* **47**, 1894–1904 (2008).
- Spiekerkoetter, U. et al. Evidence for impaired gluconeogenesis in very long-chain acyl-CoA dehydrogenase-deficient mice. *Horm. Metab. Res.* **38**, 625–630 (2006).
- Zhang, W., Della-Fera, M. A., Hartzell, D., Hausman, D. & Baile, C. Adipose tissue gene expression profiles in ob/ob mice treated with leptin. *Life Sci.* **83**, 35–42 (2008).
- Yeohor, V. K. et al. Distinct pathways of insulin-regulated versus diabetes-regulated gene expression: an *in vivo* analysis in MIRKO mice. *Proc. Natl Acad. Sci. USA* **101**, 16525–16530 (2004).
- Schwer, B., North, B. J., Frye, R. A., Ott, M. & Verdin, E. The human silent information regulator (Sir)2 homologue hSIRT3 is a mitochondrial nicotinamide adenine dinucleotide-dependent deacetylase. *J. Cell Biol.* **158**, 647–657 (2002).
- Yang, H. et al. Nutrient-sensitive mitochondrial NAD⁺ levels dictate cell survival. *Cell* **130**, 1095–1107 (2007).
- McGarry, J. D. & Foster, D. W. Regulation of hepatic fatty acid oxidation and ketone body production. *Annu. Rev. Biochem.* **49**, 395–420 (1980).
- Eaton, S., Bartlett, K. & Pourfarzam, M. Mammalian mitochondrial β -oxidation. *Biochem. J.* **320**, 345–357 (1996).
- Shibata, M., Kihara, Y., Taguchi, M., Tashiro, M. & Otsuki, M. Nonalcoholic fatty liver disease is a risk factor for type 2 diabetes in middle-aged Japanese men. *Diabetes Care* **30**, 2940–2944 (2007).
- Targher, G. et al. Nonalcoholic fatty liver disease and risk of future cardiovascular events among type 2 diabetic patients. *Diabetes* **54**, 3541–3546 (2005).
- Hsiao, P. J. et al. Significant correlations between severe fatty liver and risk factors for metabolic syndrome. *J. Gastroenterol. Hepatol.* **22**, 2118–2123 (2007).
- Kim, J. Y., Hickner, R. C., Cortright, R. L., Dohm, G. L. & Houmard, J. A. Lipid oxidation is reduced in obese human skeletal muscle. *Am. J. Physiol. Endocrinol. Metab.* **279**, E1039–E1044 (2000).
- Frerman, F. E. & Goodman, S. I. Fluorometric assay of acyl-CoA dehydrogenases in normal and mutant human fibroblasts. *Biochem. Med.* **33**, 38–44 (1985).
- Bennett, M. J. Assays of fatty acid β -oxidation activity. *Methods Cell Biol.* **80**, 179–197 (2007).

Supplementary Information is linked to the online version of the paper at www.nature.com/nature.

Acknowledgements We thank T. Canavan and J. J. Maher for primary hepatocyte preparation (P30 DK026743); C. Harris, L. Swift and the Mouse Metabolic Phenotyping Center (DK59637) for analysis of plasma and tissue lipid analysis; J. Wong for electron microscopy studies, S. Mihalik and D. Cuebas for synthesis of the 2,6-dimethylheptanoyl-CoA; A.-W. Mohsen for purification of recombinant pig ETF; Y.-C. Si for assistance with adenoviral studies; A. Wilson and J. Carroll for preparation of figures; and G. Howard and S. Ordway for editorial review. This work was supported in part by a Senior Scholarship in Aging from the Ellison Medical Foundation to E.V. and by institutional support from the J. David Gladstone Institutes. F.W.A. is an Investigator of the Howard Hughes Medical Institute and recipient of an Ellison Medical Foundation Senior Scholar Award. D.B.L. is supported by a K08 award from the National Institute on Aging and the National Institutes of Health. B.S. is supported by an Ellison Medical Foundation/AFAR Senior Postdoctoral Research Grant. N.B.R. and A.K.S. are supported by National Institutes of Health (NIH) grants PO1 HL068758-06A1, DK019514-29 and R01 DK067509-04.

Author Contributions M.D.H., T.S., E.G., E.J., B.S., C.A.G., C.H., S.B. and A.K.S. performed *in vitro*, *in vivo* and biochemical studies; O.R.I., R.D.S. and J.R.B. performed metabolomic studies; D.B.L. and Y.L. performed mass spectrometry studies; M.D.H. and E.V. designed the studies, analysed the data and wrote the manuscript; all other authors reviewed and commented on the manuscript.

Author Information Reprints and permissions information is available at www.nature.com/reprints. The authors declare no competing financial interests. Correspondence and requests for materials should be addressed to E.V. (everdin@gladstone.ucsf.edu).

METHODS

Animal studies. All animal studies were performed according to protocols approved by the Institutional Animal Care and Use Committee. Studies used wild-type and *Sirt3*^{-/-} 129Sv (as described³) male 12-week-old mice, maintained on a standard chow diet (5053 PicoLab diet; Purina), unless otherwise indicated. Mice were killed at 7:00 for fed mouse studies, or transferred to a new cage without food for 24 h from 7:00 to 7:00, and then killed for fasted mouse studies, unless otherwise indicated. Cold exposure studies were performed at 4 °C for 6 h from 7:00 to 13:00 with continuous monitoring. Core body temperature (rectal) was measured hourly with a digital thermometer (model 4600; Yellow Springs Instruments). These studies used male 4-week-old mice, either fed and given food during the cold exposure, or pre-fasted 18 h from 13:00 to 7:00 and withheld from food during the cold exposure. Glucose measurements were obtained using a handheld glucometer (FreeStyle). Concentration of ketone bodies was determined using a ketone body detection kit (Stanbio Laboratory).

Biochemical assays. Citrate synthase activity was measured by monitoring the conversion of acetyl-CoA and oxaloacetate to citrate, by the CoA-thiol reaction with 5,5'-dithio-2-nitrobenzoate (DNTB)²⁹.

Metabolomics and lipid analysis from tissue and plasma. After hepatic protein precipitation with methanol, supernatants were dried, esterified with hot, acidic methanol (acylcarnitines) or *n*-butanol (amino acids) and then analysed by tandem mass spectrometry (Quattro Micro, Waters Corporation). Acylcarnitines were assayed by adapting described methods for analysis of amino acids in dried blood spots³⁰. Organic acids were extracted in ethyl acetate, dried and then converted to their trimethyl silyl esters using N,O-bis(trimethylsilyl) trifluoroacetamide, with protection of α -keto groups by oximation with ethoxyamine hydrochloride, followed by gas chromatography mass spectrometry (Trace DSQ, Thermo Fisher Scientific)³¹. For lipid analysis, total lipids were extracted from tissue, cells or plasma by the method of Folch *et al.*³² or Bligh and Dyer³³. Individual lipid classes were separated by thin-layer chromatography on silica gel 60 A plates and visualized with rhodamine 6G. Lipid ester bands were scraped from the thin-layer chromatography plates and methylated using BF₃/methanol as described by Morrison and Smith³⁴. Concentration of ATP was determined spectrophotometrically in neutralized trichloroacetic acid filtrates by standard glucose-hexokinase assays as described previously^{35,36}.

Lipid uptake, synthesis and export methods. Fatty-acid transport was performed as described previously³⁷. Briefly [1-¹⁴C]oleic acid (58 mCi mmol⁻¹) in toluene was dried under nitrogen and resuspended in 250 μ M oleic acid/0.33% BSA in DMEM. The radiolabelled medium incubated with wild-type or *Sirt3*^{-/-} primary mouse hepatocytes for 3 min at 37 °C at which time the cells were washed extensively with PBS, lysed in 1% SDS/PBS and radioactive counts determined by scintillation counting on a Bioscan AR-2000. Triglyceride synthesis assays were performed by incubating wild-type or *Sirt3*^{-/-} primary mouse hepatocytes with [1-¹⁴C]oleic acid for 2 h. Cells were washed twice with PBS, lipids were extracted, lysates separated by thin layer chromatography, and triglyceride was quantified by radioactive counts with a Bioscan AR-2000. Export assays of very-low-density lipoprotein were performed by pre-fasting wild-type or *Sirt3*^{-/-} mice for 5 h and then injecting a tail vein with 5 mg tyloxapol. Blood samples were collected every hour for 3 h, processed for plasma and analysed for triglyceride content (Roche Trig/GB kit).

Electron microscopy. Tissues from three wild-type and three *Sirt3*^{-/-} mice were fixed by cardiac perfusion with 1.5% glutaraldehyde, 4% polyvinylpyrrolidone, 0.05% calcium chloride and 0.1 M sodium cacodylate, pH 7.4. Livers were removed, put directly into fixative, then were embedded in Epon 812 and photographed with an electron microscope (Siemens Elmiskop 101, Siemens/CTI).

Mass spectrometry. Mass spectrometry analyses were as described^{38,39}. Briefly, peptides containing acetyllysines were isolated directly from protease-digested (trypsin) mitochondrial extracts from wild-type and *Sirt3*^{-/-} mouse livers with an anti-acetyllysine-specific antibody and were identified by tandem mass spectrometry.

Immunoprecipitation. Murine liver mitochondria were prepared and purified as described⁴⁰⁻⁴². Mitochondria were lysed by sonication and resuspended in a low-stringency immunoprecipitation buffer (0.05% NP-40, 50 mM NaCl,

0.5 mM EDTA, 50 mM Tris-HCl, pH 7.4, 10 mM nicotinamide, 1 μ M trichostatin A, protease inhibitor cocktail (Roche)).

Cell culture, plasmid construction and transfection. HEK-293T cells and HeLa cells were cultured in DMEM supplemented with 10% FCS. *Acad1* (GenBank accession number BC027412) constructs were cloned into pcDNA3.1 expression vectors using standard PCR-based cloning strategies and verified by DNA sequencing. Between 5×10^6 and 1×10^7 cells (corresponding to a 10-cm culture dish) were transfected according to standard procedures either by the CaPO₄ coprecipitation method or by lipofection (Invitrogen). Cells were maintained in growth medium for 24–48 h before collection. To monitor *in vivo* SIRT3 deacetylation or co-immunoprecipitation, LCAD-Flag expression vectors were co-transfected with an empty pcDNA3.1 vector, SIRT3-HA, catalytically inactive SIRT3-H248Y-HA, SIRT4-HA or SIRT5-HA and then immunoprecipitated with anti-Flag or anti-HA antiserum and probed for acetylation or co-immunoprecipitation, as described previously¹⁹.

Adenovirus preparation and murine injection. Murine *Sirt3* complementary DNA was cloned into pShuttle-IRES-GFP-1 vector (Stratagene), or an empty vector as a negative control. Adenoviruses were recombined and produced using pAdeasy Adenoviral System (Stratagene). After amplification with Ad-293 packaging cell line, virus was purified using caesium chloride gradient ultracentrifugation and dialysed into PBS plus 10% glycerol as described⁴³. 12-week-old male mice were injected in a tail vein with adenovirus overexpressing either GFP (control) or SIRT3 at dose of 5×10^9 plaque-forming units per gram of body mass, as described⁴⁴. The mice were monitored for signs of distress, and recovered under observation. On the sixth day after injection of the virus, the mice were killed and their livers removed and measured for fatty-acid oxidation assays, as described earlier.

Statistical analyses. Results are given as the mean \pm standard error. Statistical analyses represent a non-parametric Student's *t*-test, and null hypotheses were rejected at $P < 0.05$.

29. Srere, P. A. Citrate synthase. *Methods Enzymol.* **13**, 3–11 (1969).
30. Wu, J. Y. *et al.* ENU mutagenesis identifies mice with mitochondrial branched-chain aminotransferase deficiency resembling human maple syrup urine disease. *J. Clin. Invest.* **113**, 434–440 (2004).
31. Jensen, M. V. *et al.* Compensatory responses to pyruvate carboxylase suppression in islet β -cells. Preservation of glucose-stimulated insulin secretion. *J. Biol. Chem.* **281**, 22342–22351 (2006).
32. Folch, J., Lees, M. & Sloane Stanley, G. H. A simple method for the isolation and purification of total lipides from animal tissues. *J. Biol. Chem.* **226**, 497–509 (1957).
33. Bligh, E. G. & Dyer, W. J. A rapid method of total lipid extraction and purification. *Can. J. Biochem. Physiol.* **37**, 911–917 (1959).
34. Morrison, W. R. & Smith, L. M. Preparation of fatty acid methyl esters and dimethylacetals from lipids with boron fluoride-methanol. *J. Lipid Res.* **5**, 600–608 (1964).
35. Oliver, H. & Lowry, J. V. P. *A Flexible System of Enzymatic Analysis* (Academic Press, 1972).
36. Saha, A. K. *et al.* Pioglitazone treatment activates AMP-activated protein kinase in rat liver and adipose tissue *in vivo*. *Biochem. Biophys. Res. Commun.* **314**, 580–585 (2004).
37. Stremmel, W. & Berk, P. D. Hepatocellular influx of [¹⁴C]oleate reflects membrane transport rather than intracellular metabolism or binding. *Proc. Natl Acad. Sci. USA* **83**, 3086–3090 (1986).
38. Rikova, K. *et al.* Global survey of phosphotyrosine signaling identifies oncogenic kinases in lung cancer. *Cell* **131**, 1190–1203 (2007).
39. Rush, J. *et al.* Immunoaffinity profiling of tyrosine phosphorylation in cancer cells. *Nature Biotechnol.* **23**, 94–101 (2005).
40. Graham, J. M. Isolation of mitochondria from tissues and cells by differential centrifugation. *Curr. Protocols Cell Biol.* (suppl. 4), unit 3.3 (1999).
41. Graham, J. M. Purification of a crude mitochondrial fraction by density-gradient centrifugation. *Curr. Protocols Cell Biol.* (suppl. 4), unit 3.4 (1999).
42. Hirschey, M. D., Shimazu, T., Huang, J. & Verdin, E. Acetylation of mitochondrial proteins. *Methods Enzymol.* **457**, 137–147 (2009).
43. Taniguchi, C. M., Ueki, K. & Kahn, R. Complementary roles of IRS-1 and IRS-2 in the hepatic regulation of metabolism. *J. Clin. Invest.* **115**, 718–727 (2005).
44. Ueki, K., Kondo, T., Tseng, Y. H. & Kahn, C. R. Central role of suppressors of cytokine signaling proteins in hepatic steatosis, insulin resistance, and the metabolic syndrome in the mouse. *Proc. Natl Acad. Sci. USA* **101**, 10422–10427 (2004).